

Analysis of the semileptonic $B \rightarrow K_1 \ell^+ \ell^-$ transitions and non-leptonic $B \rightarrow K_1 \gamma$ decay in the AdS/QCD correspondence

S. Momeni*, R. Khosravi†

Department of Physics, Isfahan University of Technology, Isfahan 84156-83111, Iran

We consider the axial-vector mesons $K_1(1270)$ and $K_1(1400)$ as a mixture of two $|^3P_1\rangle$ and $|^1P_1\rangle$ states with the mixing angle θ that equal to $(-34 \pm 13)^\circ$. We calculate the light-front distribution amplitudes (LFDAs) and decay constant formulas for both the axial-vector mesons K_1 in the AdS/QCD correspondence. The transition form factors of the semileptonic $B \rightarrow K_1$ decays are derived in terms of the LFDAs for K_1 mesons. Using these form factors and decay constant values, the differential branching ratios of $B \rightarrow K_1(1270, 1400) \ell^+ \ell^-$, $\ell = \mu, \tau$ transitions are plotted with respect to the four-momentum transfer squared, q^2 . In addition, the branching ratio values of these decays and the non-leptonic $B \rightarrow K_1(1270, 1400) \gamma$ decays are estimated. A comparison is made between our results for the branching ratios of $B \rightarrow K_1(1270, 1400) \gamma$ decays in the AdS/QCD model and predictions obtained from the light-cone sum rules (LCSR) as well as the experimental values. Finally, the forward-backward asymmetries for the aforementioned semileptonic decays are plotted on q^2 in both the AdS/QCD correspondence and two Higgs doublet model (2HDM) in order to test the standard model (SM) and search for the new physics (NP).

I. INTRODUCTION

Inclusive and exclusive decays of B meson improve our studies in understanding the dynamics of quantum chromodynamics (QCD). Among of all B decays, the theoretical description of the semileptonic decays is relatively simple. These semileptonic decays usually occur by two various diagrams: a) simple tree diagrams which can be performed via the weak interaction, b) electroweak penguin and box diagrams which can be fulfilled through the flavor changing neutral current (FCNC) transitions in the SM. The FCNC decays $B \rightarrow K_1 \ell^+ \ell^-$, involving the axial-vector strange mesons, have been the subjects of many theoretical studies, since they are important for a few reasons. They are sensitive to NP contributions to penguin operators. Therefore, we can check the SM and search NP by estimating the SM predictions for these decays and comparing these results to the corresponding values from some NP models. On the other hand, in particle physics, reliable calculations of heavy-to-light transition form factors of semileptonic B decays are very important since they are also used to determine the amplitude of non-leptonic B decays applied to evaluate the CKM parameters as well as to test various properties of the SM.

Sofar, the heavy-to-light transitions $B \rightarrow K_1 \ell^+ \ell^-$, as a FCNC process, have been studied in many theoretical approaches in the frame work of the SM such as the three-point QCD sum rules (3PSR) [1, 2], the LCSR [3–5], perturbative QCD (PQCD) approach [6, 7] and light-front quark model (LFQM) [8, 9]; and some NP models, such as universal extra dimension [10–12], models involving supersymmetry [13], the fourth-generation fermions [14], the 2HDM [15], the non-universal Z' model [16] and the model-independent new-physics corrections to the Wilson coefficients [17]. Considering the physical observables of these decays, such as the branching ratio value, dilepton invariant mass spectrum, forward-backward asymmetry and double lepton polarization provide us a lot of useful information. In this paper, we plan to investigate the FCNC $B \rightarrow K_1$ transitions in the AdS/QCD correspondence.

The interactions among quarks and gluons, described by QCD, are particularly important because they exhibit many characteristic and challenging features of a strongly-coupled theory. In the high momentum transfer regime, QCD is asymptotically free and can be considered with methods of perturbation theory. In the low momentum transfer regime, confinement is created and QCD becomes strongly-coupled. Therefore, one of the most important issues of strong interaction dynamics is to obtain analytic solutions for the wave functions of hadrons outside of the perturbative regime. One of the proposed ideas for overcoming these problems is based on the light-front QCD and using the AdS/CFT correspondence [18, 19] between string states in anti-de Sitter (AdS) space and conformal field theories (CFT) in physical space-time [20–25]. The application of the AdS space and conformal methods to QCD can be motivated from the experimental evidence [26], and theoretical discussions that the QCD coupling $\alpha_s(Q^2)$ has an infrared fixed point at low Q^2 [27, 28]. In this region, the AdS/QCD approach has been successful in obtaining general properties of phenomenological QCD such as hadronic spectra, decay constants, and wave functions [29–32].

There is a significant mapping between the AdS space description of hadrons and the light-front wave functions

* e-mail: samira.momeni@phy.iut.ac.ir

† e-mail: rezakhosravi @ cc.iut.ac.ir

(LFWFs) of bound states in QCD quantized on the light-front, known as holographic LFWFs (for instance see [25]). The LFWFs in QCD, similar to the Schrodinger wave functions of atomic physics, provide an explanation of the structure and internal dynamics of hadrons in terms of their constituent quarks and gluons. However, they are determined at fixed light-front time instead of at fixed ordinary time [28]. Using the LFWF, some physical quantities related to hard exclusive reactions can be calculated such as distribution amplitudes, form factors and structure functions.

The holographic LFWF has been successfully applied to describe diffractive ρ meson electroproduction at HERA [33]. In addition, this LFWF has been used to study the spectrum [34] and the distribution amplitudes (DAs) of light and heavy mesons [35]. After introducing the light-front spinor structure of the wave functions for light vector mesons in analogy with that of the photon, light-front distribution amplitudes (LFDAs) of the ρ and K^* vector mesons have been predicted in $B \rightarrow \rho\gamma$ [36], and $B \rightarrow K^*\gamma$ [37] decays. Also, using the holographic DAs, the transition form factors of the semileptonic $B \rightarrow \rho$ [38], and $B \rightarrow K^*$ decays [39] have been estimated. These form factors have been then utilized to make predictions for the isospin asymmetry of $B \rightarrow K^*\mu^+\mu^-$ transition [40] and for branching ratio values of the semileptonic $B \rightarrow \rho\ell\nu$ decays [41]. Dynamical spin effects have been taken into account of the holographic pion wave function in order to predict its mean charge radius, decay constant, space-like electromagnetic form factor, twist-2 DA and the photon-to-pion transition form factor [42]. Recently, the AdS/QCD DAs of pseudoscalar mesons and their application to B -meson decays have been studied in Ref. [43, 44].

Sofar, the holographic DAs have been not calculated for axial-vector mesons. The study of the DAs for axial-vector mesons is important for considering exclusive decays such as $B \rightarrow K_1(1270)\gamma$. The branching ratio value of the aforementioned decay has been measured by Belle [45], whereas the axial-vector meson $K_1(1270)$ is a mixtures of two $|^3P_1\rangle$ and $|^1P_1\rangle$ states. Usually, the DAs for light mesons are estimated from the LCSR method, known as light-cone distribution amplitudes (LCDAs). In this work, we plan to calculate the holographic DAs and tensor decay constants for the axial-vector mesons $K_1(1270)$ and $K_1(1400)$. Due to the axial-vector mesons K_1 are considered as a mixture of two states, we need to investigate the holographic DAs for $|K_{1A}\rangle$ and $|K_{1B}\rangle$ states in the AdS/QCD correspondence in terms of the LFWFs. Then, we can derive the DAs for K_1 mesons in terms of the holographic DAs for these states. Inserting the holographic DAs for K_1 in the transition form factor equations of the semileptonic $B \rightarrow K_1$ decays, which have been calculated via the LCSR method [5], we can predict the branching ratio value for $B \rightarrow K_1(1270)\gamma$ decay.

The main purpose of this work is as follows:

- Investigation of the holographic DAs for the axial-vector mesons $K_1(1270)$ and $K_1(1400)$ in the AdS/QCD correspondence. It would be reminded that an accurate calculation of the DAs is very important since they provide a major source of uncertainty in the theoretical predictions of the physical quantities.
- Calculation of the tensor decay constants for the axial-vector mesons $K_1(1270, 1400)$ and considering the form factors of $B \rightarrow K_1(1270, 1400)\ell^+\ell^-$ decays in order to investigation the dilepton invariant mass spectrums and prediction of the branching ratio values of them.
- Predictions of the branching ratio values for the non-leptonic $B \rightarrow K_1(1270, 1400)\gamma$ decays. A comparison is made between our result for $B \rightarrow K_1(1270)\gamma$ decay and the experimental value.
- Considering the forward-backward asymmetries for $B \rightarrow K_1(1270, 1400)\ell^+\ell^-$ transitions on q^2 in the AdS/QCD correspondence and 2HDM in order to test the SM and search for the NP.

The contents of this paper are as follows: In section II, the LFWFs for the axial-vector mesons $K_1(1270, 1400)$ are calculated in the frame work of the AdS/QCD. Then, the decay constant formulas and LFDAs for K_1 are derived. For this purpose, we investigate the holographic DAs for $|K_{1A}\rangle$ and $|K_{1B}\rangle$ states in the AdS/QCD correspondence in terms of the LFWFs. In section III, we analyze the LFDAs and decay constants for K_1 mesons and compare our results with predictions of the LCSR method. Applying the LFDAs of K_1 mesons in the transition form factors of the FCNC $B \rightarrow K_1$ decays, we analyze these form factors as well as the dilepton invariant mass spectrum on q^2 . In addition, we obtain the branching ratio values for $B \rightarrow K_1(1270, 1400)\ell^+\ell^-$ and $B \rightarrow K_1(1270, 1400)\gamma$ decays. Our result for the branching ratio of the non-leptonic decay $B \rightarrow K_1(1270)\gamma$ is compared with the experimental value. Finally, the forward-backward asymmetries for $B \rightarrow K_1(1270, 1400)\ell^+\ell^-$ transitions, with respect to q^2 , are compared in the AdS/QCD correspondence and 2HDM.

II. DISTRIBUTION AMPLITUDES AND DECAY CONSTANTS IN ADS/QCD

The physical states of $K_1(1270)$ and $K_1(1400)$ mesons are considered as a mixture of two $|^3P_1\rangle$ and $|^1P_1\rangle$ states and can be parameterized in terms of a mixing angle θ_K , as follows:

$$\begin{aligned} |K_1(1270)\rangle &= \sin\theta_K|^3P_1\rangle + \cos\theta_K|^1P_1\rangle, \\ |K_1(1400)\rangle &= \cos\theta_K|^3P_1\rangle - \sin\theta_K|^1P_1\rangle, \end{aligned} \quad (1)$$

where $|^3P_1\rangle \equiv |K_{1A}\rangle$ and $|^1P_1\rangle \equiv |K_{1B}\rangle$ have different masses and decay constants. Also, the mixing angle θ_K can be determined by the experimental data. There are various approaches to estimate the mixing angle. The result $35^\circ \leq |\theta_K| \leq 55^\circ$ was found in Ref. [46], while two possible solutions were obtained as $|\theta_K| \approx 33^\circ \vee 57^\circ$ in Ref. [47] and as $|\theta_K| \approx 37^\circ \vee 58^\circ$ in Ref. [48]. A new window for the value of θ_K is estimated from the result of $\tau \rightarrow K_1(1270)\nu_\tau$ data as [49]

$$\theta_K = -(34 \pm 13)^\circ. \quad (2)$$

Sofar this value is used in Refs. [1, 2, 4, 13, 15, 17]. In this study, we also use the result of $\theta_K = -(34 \pm 13)^\circ$.

The twist-2 DAs, $\Phi_{K_1}^{\parallel,\perp}$, for K_1 mesons are given in terms of the twist-2 DAs of K_{1A} and K_{1B} states, $\Phi_{K_{1A}}^{\parallel,\perp}(u)$ and $\Phi_{K_{1B}}^{\parallel,\perp}(u)$, as [3]:

$$\begin{aligned} \Phi_{K_1}^{\parallel}(u) &= C_1 \frac{f_{K_{1A}} m_{K_{1A}}}{f_{K_1} m_{K_1}} \Phi_{K_{1A}}^{\parallel}(u) + C_2 \frac{f_{K_{1B}} m_{K_{1B}}}{f_{K_1} m_{K_1}} \Phi_{K_{1B}}^{\parallel}(u), \\ \Phi_{K_1}^{\perp}(u) &= C_1 \frac{f_{K_{1A}}^{\perp}}{f_{K_1}^{\perp}} \Phi_{K_{1A}}^{\perp}(u) + C_2 \frac{f_{K_{1B}}^{\perp}}{f_{K_1}^{\perp}} \Phi_{K_{1B}}^{\perp}(u), \end{aligned} \quad (3)$$

where $(C_1, C_2) = (\sin \theta_K, \cos \theta_K)$ for $K_1(1270)$ meson, and $(C_1, C_2) = (\cos \theta_K, -\sin \theta_K)$ for $K_1(1400)$. In this phrases, u refer to the momentum fraction carried by the quark in K_1 . In addition, f_{K_1} and $f_{K_1}^{\perp}$ are decay constants, written in terms of $f_{K_{1A(1B)}}$ and $f_{K_{1A(1B)}}^{\perp}$ as

$$\begin{aligned} f_{K_1} &= C_1 \frac{m_{K_{1A}}}{m_{K_1(1270)}} f_{K_{1A}} + C_2 \frac{m_{K_{1B}}}{m_{K_1(1270)}} a_0^{\parallel, K_{1B}} f_{K_{1B}}, \\ f_{K_1}^{\perp} &= C_1 a_0^{\perp, K_{1A}} f_{K_{1A}}^{\perp} + C_2 f_{K_{1B}}^{\perp}, \end{aligned} \quad (4)$$

where $a_0^{\perp, K_{1A}}$ and $a_0^{\parallel, K_{1B}}$ are G-parity invariant Gegenbauer moments for K_{1A} and K_{1B} states which have been estimated in Ref. [3].

First, we aim to calculate the twist-2 DAs for K_1 mesons in the AdS/QCD correspondence. According to Eq. (3), we need to investigate the twist-2 DAs for two states K_{1A} and K_{1B} in terms of the holographic LFWFs. In order to consider the twist-2 DAs, the matrix elements of K_{1A} and K_{1B} states should be considered. For instance, the following two-particle matrix elements of state K_{1A} in the light-front coordinate, $x^\mu = (x^+, x^-, \mathbf{x}_\perp)$, at equal light-front time x^+ , are written as:

$$\langle 0 | \bar{u}(0) \gamma^\mu \gamma_5 s(x^-) | K_{1A}(p, \lambda) \rangle = f_{K_{1A}} m_{K_{1A}} \int_0^1 du e^{-iup^+ x^-} \{ p^\mu \frac{\varepsilon_\lambda \cdot x}{p^+ x^-} \Phi_{K_{1A}}^{\parallel}(u, \mu) + \dots \}, \quad (5)$$

$$\langle 0 | \bar{u}(0) \sigma^{\mu\nu} \gamma_5 s(x^-) | K_{1A}(p, \lambda) \rangle = i f_{K_{1A}}^{\perp} \int_0^1 du e^{-iup^+ x^-} \{ (\varepsilon_\lambda^\mu p^\nu - \varepsilon_\lambda^\nu p^\mu) \Phi_{K_{1A}}^{\perp}(u, \mu) + \dots \}, \quad (6)$$

where $\gamma^\mu = (\gamma^+, \gamma^-, \gamma^1, \gamma^2)$. The "..." describes the contributions coming from higher twist DAs. In these relations, p^+ is the "plus" component of the four-momentum of K_{1A} state given by $p^\mu = \left(p^+, \frac{m_{K_{1A}}^2}{p^+}, 0_\perp \right)$. The polarization

vectors ε_λ ($\lambda = L, T$) for state K_{1A} are chosen as $\varepsilon_L = \left(\frac{p^+}{m_{K_{1A}}}, \frac{m_{K_{1A}}}{p^+}, 0_\perp \right)$, and $\varepsilon_{T(\pm)} = \frac{1}{\sqrt{2}} (0, 0, 1, \pm i)$.

Taking $\lambda = L$ and $\mu = +$ in Eq. (5), in addition, the scalar product of Eq. (6) in $(\varepsilon_T^*)_\mu$, we obtain:

$$\langle 0 | \bar{u}(0) \gamma^+ \gamma_5 s(x^-) | K_{1A}(p, L) \rangle = f_{K_{1A}} m_{K_{1A}} \int_0^1 du e^{-iup^+ x^-} [p^+ \left(\frac{\varepsilon_L \cdot x}{p^+ x^-} \right) \Phi_{K_{1A}}^{\parallel}(u, \mu)], \quad (7)$$

$$\langle 0 | \bar{u}(0) [\gamma \cdot \varepsilon_T^*, \gamma^+] \gamma_5 s(x^-) | K_{1A}(p, \pm) \rangle = 2 f_{K_{1A}}^{\perp} \int_0^1 du e^{-iup^+ x^-} [p^+ (\varepsilon_T^1 \mp i \varepsilon_T^2) \Phi_{K_{1A}}^{\perp}(u, \mu)], \quad (8)$$

where $\gamma \cdot \varepsilon_T^*$ is placed instead of $\gamma_1 \mp i \gamma_2$. Applying the Fourier transform of the above matrix elements with respect to the longitudinal distance x^- , the twist-2 DAs are given by:

$$\Phi_{K_{1A}}^{\parallel}(\alpha, \mu) = \frac{1}{f_{K_{1A}}} \int dx^- e^{i\alpha p^+ x^-} \langle 0 | \bar{u}(0) \gamma^+ \gamma_5 s(x^-) | K_{1A}(p, L) \rangle, \quad (9)$$

$$\Phi_{K_{1A}}^{\perp}(\alpha, \mu) = \frac{1}{2 f_{K_{1A}}^{\perp}} \int dx^- e^{i\alpha p^+ x^-} \langle 0 | \bar{u}(0) [\gamma \cdot \varepsilon_T^*, \gamma^+] \gamma_5 s(x^-) | K_{1A}(p, \pm) \rangle, \quad (10)$$

where α is the momentum fraction of quark in state K_{1A} .

To obtain $\Phi_{K_{1A}}^{\parallel,\perp}$ in Eqs. (9) and (10), we should calculate the matrix elements which appear in these relations. These matrix elements can be estimated by using the LFWF, $\Psi_{h,\bar{h}}^{K_{1A},\lambda}(\alpha, \mathbf{k})$ of the K_{1A} state as [50]:

$$p^+ \int dx^- e^{i\alpha p^+ x^-} \langle 0 | \bar{u}(0) \Gamma s(x^-) | K_{1A}(p, \lambda) \rangle = \sqrt{\frac{N_c}{4\pi}} \sum_{h,\bar{h}} \int^{|\mathbf{k}| < \mu} \frac{d^2 \mathbf{k}}{(2\pi)^2} \Psi_{h,\bar{h}}^{K_{1A},\lambda}(\alpha, \mathbf{k}) \times \left\{ \frac{\bar{v}_{\bar{h}}((1-\alpha)p^+, -\mathbf{k})}{\sqrt{(1-\alpha)}} \Gamma \frac{u_h(\alpha p^+, \mathbf{k})}{\sqrt{\alpha}} \right\}, \quad (11)$$

while Γ stands for $\gamma^+ \gamma_5$ and $[\gamma \cdot \varepsilon_T^*, \gamma^+] \gamma_5$. Here \mathbf{k} is transverse momenta of quark, and the renormalization scale μ is identified with the ultraviolet cut-off on \mathbf{k} [51, 52]. Also, $u(\bar{v})$ and $h(\bar{h})$ are the spinor and helicity of quark (anti-quark), respectively. The explicit expressions for light-front spinors with positive and negative helicities have been given in Ref. [53]. Using these expressions for the light-front spinors $\bar{v}_{\bar{h}}$ and u_h , We obtain:

$$\frac{\bar{v}_{\bar{h}}}{\sqrt{(1-\alpha)}} \gamma^+ \gamma_5 \frac{u_h}{\sqrt{\alpha}} = p^+ (\delta_{\bar{h}+, h-} - \delta_{\bar{h}-, h+}), \quad (12)$$

$$\frac{\bar{v}_{\bar{h}}}{\sqrt{(1-\alpha)}} [\varepsilon_{\pm}^* \cdot \gamma, \gamma^+] \gamma_5 \frac{u_h}{\sqrt{\alpha}} = \mp 4\sqrt{2} p^+ \delta_{h\pm, \bar{h}\pm}, \quad (13)$$

where $h+$ and $h-$ are used for positive and negative helicity, respectively. The LFWF of K_{1A} in Eq. (11) is defined in momenta space as [50]:

$$\Psi_{h,\bar{h}}^{K_{1A},\lambda}(\alpha, \mathbf{k}) = \sqrt{\frac{N_c}{4\pi}} S_{h,\bar{h}}^{K_{1A},\lambda}(\alpha, \mathbf{k}) \phi_{\lambda}^{K_{1A}}(\alpha, \mathbf{k}). \quad (14)$$

In Refs. [36, 37], the helicity-dependent part of the LFWF for vector meson K^* has been chosen as: $S_{h,\bar{h}}^{K^*,\lambda}(\alpha, \mathbf{k}) = \frac{\bar{u}_h((1-\alpha)p^+, -\mathbf{k})}{\sqrt{(1-\alpha)}} (\gamma \cdot \varepsilon_{\lambda}^*) \frac{v_{\bar{h}}(\alpha p^+, \mathbf{k})}{\sqrt{\alpha}}$, in analogy with vector meson, we propose $S_{h,\bar{h}}^{K_{1A},\lambda}$ for the axial-vector state K_{1A} as:

$$S_{h,\bar{h}}^{K_{1A},\lambda}(\alpha, \mathbf{k}) = \frac{\bar{u}_h((1-\alpha)p^+, -\mathbf{k})}{\sqrt{(1-\alpha)}} (\gamma \cdot \varepsilon_{\lambda}^*) \gamma_5 \frac{v_{\bar{h}}(\alpha p^+, \mathbf{k})}{\sqrt{\alpha}}. \quad (15)$$

After some calculations and using expressions for \bar{u}_h and $v_{\bar{h}}$ in light-front coordinate, we extract the factor $S_{h,\bar{h}}^{K_{1A},\lambda}(\alpha, \mathbf{k})$ as

$$S_{h,\bar{h}}^{K_{1A},\pm}(\alpha, \mathbf{k}) = \pm \frac{\sqrt{2}}{\alpha(1-\alpha)} \left\{ [(1-\alpha)\delta_{h\mp, \bar{h}\pm} + \alpha\delta_{h\pm, \bar{h}\mp}] k e^{\pm i\theta_k} - [(1-\alpha)m_u - \alpha m_{\bar{s}}] \delta_{h\pm, \bar{h}\pm} \right\},$$

$$S_{h,\bar{h}}^{K_{1A},L}(\alpha, \mathbf{k}) = -\frac{1}{m_{K_{1A}} \alpha(1-\alpha)} \left\{ [\alpha(1-\alpha)m_{K_{1A}}^2 + \mathbf{k}^2 - m_u m_{\bar{s}}] (\delta_{h-, \bar{h}+} - \delta_{h+, \bar{h}-}) \right.$$

$$\left. + k[m_u + m_{\bar{s}}] (e^{-i\theta_k} \delta_{h+, \bar{h}+} + e^{i\theta_k} \delta_{h-, \bar{h}-}) \right\}. \quad (16)$$

In this relation, we have used the polar representation of the transverse momentum, i.e. $\mathbf{k} = k e^{i\theta_k}$. Using Eqs. (12), (13) and (16), we can rewrite Eqs. (9) and (10) as:

$$\Phi_{K_{1A}}^{\parallel}(\alpha, \mu) = \frac{N_c}{\pi f_{K_{1A}} m_{K_{1A}}} \int^{|\mathbf{k}| < \mu} \frac{d^2 \mathbf{k}}{(2\pi)^2} [\alpha(1-\alpha)m_{K_{1A}}^2 - m_u m_{\bar{s}} + \mathbf{k}^2] \frac{\phi_L^{K_{1A}}(\alpha, \mathbf{k})}{\alpha(1-\alpha)}, \quad (17)$$

$$\Phi_{K_{1A}}^{\perp}(\alpha, \mu) = \frac{N_c}{2\pi f_{K_{1A}}^{\perp}} \int^{|\mathbf{k}| < \mu} \frac{d^2 \mathbf{k}}{(2\pi)^2} [(1-\alpha)m_u - \alpha m_{\bar{s}}] \frac{\phi_T^{K_{1A}}(\alpha, \mathbf{k})}{\alpha(1-\alpha)}. \quad (18)$$

Inserting the Fourier transform relations as

$$\phi_{\lambda}(\alpha, \mathbf{k}) = \int d^2 \mathbf{r} e^{-i\mathbf{k} \cdot \mathbf{r}} \phi_{\lambda}(\alpha, \mathbf{r}), \quad \mathbf{k}^2 \phi_{\lambda}(\alpha, \mathbf{k}) = \int d^2 \mathbf{r} e^{-i\mathbf{k} \cdot \mathbf{r}} (-\nabla^2) \phi_{\lambda}(\alpha, \mathbf{r}),$$

into Eqs. (17) and (18) and using relations such as $\int_0^{2\pi} e^{-ikr\cos\theta} d\theta = 2\pi J_0(kr)$, and $\int_0^\mu k J_0(kr) dk = \mu/r J_1(\mu r)$, where J_0 and J_1 are Bessel functions, we obtain the following expressions for the twist-2 DAs of K_{1A} state as:

$$\Phi_{K_{1A}}^\parallel(\alpha, \mu) = \frac{N_c}{\pi f_{K_{1A}} m_{K_{1A}}} \int dr \mu J_1(\mu r) [\alpha(1-\alpha) m_{K_{1A}}^2 - m_u m_{\bar{s}} - \nabla_r^2] \frac{\phi_L^{K_{1A}}(r, \alpha)}{\alpha(1-\alpha)}, \quad (19)$$

$$\Phi_{K_{1A}}^\perp(\alpha, \mu) = \frac{N_c}{\pi f_{K_{1A}}^\perp} \int dr \mu J_1(\mu r) [(1-\alpha) m_u - \alpha m_{\bar{s}}] \frac{\phi_T^{K_{1A}}(r, \alpha)}{\alpha(1-\alpha)}. \quad (20)$$

Similarly, we can estimate the twist-2 DAs for K_{1B} state as

$$\Phi_{K_{1B}}^\parallel(\alpha, \mu) = \frac{N_c}{\pi f_{K_{1B}}^\perp} \int dr \mu J_1(\mu r) [(1-\alpha) m_u - \alpha m_{\bar{s}}] \frac{\phi_L^{K_{1B}}(r, \alpha)}{\alpha(1-\alpha)}, \quad (21)$$

$$\Phi_{K_{1B}}^\perp(\alpha, \mu) = \frac{N_c}{\pi f_{K_{1B}} m_{K_{1B}}} \int dr \mu J_1(\mu r) [\alpha(1-\alpha) m_{K_{1B}}^2 - m_u m_{\bar{s}} - \nabla_r^2] \frac{\phi_T^{K_{1B}}(r, \alpha)}{\alpha(1-\alpha)}. \quad (22)$$

Having the twist-2 DAs, we can obtain the twist-3 DAs $g_\perp^{(a)}$, $g_\perp^{(v)}$, $h_\parallel^{(t)}$ and $h_\parallel^{(p)}$ by Wandzura-Wilczek-type relations as [54]

$$\begin{aligned} g_\perp^{(a)}(u) &\simeq \frac{1}{2} \left[\int_0^u dv \frac{\Phi^\parallel(v)}{\bar{v}} + \int_u^1 dv \frac{\Phi^\parallel(v)}{v} \right], \\ g_\perp^{(v)}(u) &\simeq 2 \left[\bar{u} \int_0^u dv \frac{\Phi^\parallel(v)}{\bar{v}} + u \int_u^1 dv \frac{\Phi^\parallel(v)}{v} \right], \\ h_\parallel^{(t)}(u) &= \xi \left[\int_0^u dv \frac{\Phi^\perp(v)}{\bar{v}} - \int_u^1 dv \frac{\Phi^\perp(v)}{v} \right], \\ h_\parallel^{(p)}(u) &= 2 \left[\bar{u} \int_0^u dv \frac{\Phi^\perp(v)}{\bar{v}} + u \int_u^1 dv \frac{\Phi^\perp(v)}{v} \right], \end{aligned} \quad (23)$$

where $\xi = 2u - 1$ and $\bar{u} = 1 - u$.

Now, we are also able to calculate the decay constants in terms of the LFWFs. The G-parity conserving decay constants of the axial vector-states are defined as:

$$\langle 0 | \bar{u}(0) \gamma^\mu \gamma^5 s(0) | K_{1A}(p, \lambda) \rangle = -i f_{K_{1A}} m_{K_{1A}} \varepsilon_\lambda^\mu, \quad (24)$$

$$\langle 0 | \bar{u}(0) \sigma^{\mu\nu} \gamma^5 s(0) | K_{1B}(p, \lambda) \rangle = -f_{K_{1B}}^\perp (\varepsilon_\lambda^\mu p^\nu - \varepsilon_\lambda^\nu p^\mu), \quad (25)$$

and we take $f_{K_{1A}}^\perp = f_{K_{1A}}$, $f_{K_{1B}} = f_{K_{1B}}^\perp$ in $\mu = 1$ GeV [3, 4]. After expanding the left-hand-sides of Eqs. (24) and (25) the same way as before, we obtain the decay constants as follows:

$$f_{K_{1A}} = \frac{N_c}{m_{K_{1A}} \pi} \int_0^1 d\alpha [\alpha(1-\alpha) m_{K_{1A}}^2 - m_u m_{\bar{s}} - \nabla_r^2] \frac{\phi_L^{K_{1A}}(r, \alpha)}{\alpha(1-\alpha)} \Big|_{r=0}, \quad (26)$$

$$f_{K_{1B}}^\perp = \frac{N_c}{m_{K_{1B}} \pi} \int_0^1 d\alpha [\alpha(1-\alpha) m_{K_{1B}}^2 - m_u m_{\bar{s}} - \nabla_r^2] \frac{\phi_L^{K_{1B}}(r, \alpha)}{\alpha(1-\alpha)} \Big|_{r=0}. \quad (27)$$

To specify $\phi_\lambda^{K_{1A}(K_{1B})}(r, \alpha)$ which includes dynamical properties of K_{1A} (or K_{1B}) in the LFWF in Eq. (14), we are going to use the AdS/QCD. Based on a first semiclassical approximation to the light-front QCD, with massless quarks, the function ϕ_λ can be factorized as [28]

$$\phi_\lambda(\zeta, \alpha, \theta) = \mathcal{N}_\lambda \frac{\psi(\zeta)}{\sqrt{2\pi\zeta}} f(\alpha) e^{iL\theta}, \quad (28)$$

where \mathcal{N}_λ is a normalization constant which depends on polarization of the axial-vector meson. In this relation, L is the orbital angular momentum quantum number and variable $\zeta = \sqrt{\alpha(1-\alpha)} r$, where r is the transverse distance between the quark and anti-quark forming the meson. The function $\psi(\zeta)$ satisfies the so-called holographic light-front Schroedinger equation as

$$\left(-\frac{d^2}{d\zeta^2} - \frac{1-4L^2}{4\zeta^2} + U(\zeta) \right) \psi(\zeta) = M^2 \psi(\zeta), \quad (29)$$

where M is hadron bound-state mass and $U(\zeta)$ is the effective potential which involves all the complexity of the interaction terms in the QCD Lagrangian.

According to the AdS/QCD, the holographic light-front Schroedinger equation maps onto the wave equation for strings propagating in AdS space if ζ is identified with the fifth dimension in AdS_5 . To illustrate this issue, we start with the generalized Proca action in AdS_5 as [55]

$$S = \int d^4x dz \sqrt{g} e^{\varphi(z)} \left(\frac{1}{4} g^{MR} g^{NS} F_{MN} F_{RS} - \frac{1}{2} \mu^2 g^{MN} \Phi_M \Phi_N \right), \quad (30)$$

where $g = \left(\frac{R}{z}\right)^{10}$ is the modulus of the determinant of the metric tensor g_{MN} . The mass μ in Eq. (30) is not a physical observable. $\Phi_M(x, z)$ is a vector field and $F_{MN} = \partial_M \Phi_N - \partial_N \Phi_M$. In this action, the dilaton background $\varphi(z)$ is only a function of the holographic variable z which vanishes if $z \rightarrow \infty$. Variation of Eq. (30) leads to the system of coupled differential equations of motion as

$$\left[\partial_\mu \partial^\mu - \frac{z^3}{e^{\varphi(z)}} \partial_z \left(\frac{e^{\varphi(z)}}{z^3} \partial_z \right) - \partial_z^2 \varphi + \frac{(\mu R)^2}{z^2} - 3 \right] \Phi_z = 0, \quad (31)$$

$$\left[\partial_\mu \partial^\mu - \frac{z}{e^{\varphi(z)}} \partial_z \left(\frac{e^{\varphi(z)}}{z} \partial_z \right) + \frac{(\mu R)^2}{z^2} \right] \Phi_\nu = -\frac{2}{z} \partial_\nu \Phi_z. \quad (32)$$

Imposing the condition $\Phi_z = 0$ which means physical hadrons have no polarization in the z direction, the wave equation is obtained as

$$\left[\partial_\mu \partial^\mu - \frac{z}{e^{\varphi(z)}} \partial_z \left(\frac{e^{\varphi(z)}}{z} \partial_z \right) + \left(\frac{\mu R}{z} \right)^2 \right] \Phi_\nu = 0. \quad (33)$$

A free spin-1 hadronic state in holographic QCD is described by a plane wave in physical space-time with polarization components $\epsilon_\nu(p)$ along the physical coordinates and a z -dependent profile function $\Phi_\nu(x, z) = e^{ip \cdot x} \Phi(z) \epsilon_\nu(p)$, with invariant mass $p_\mu p^\mu = M^2$. Inserting $\Phi_\nu(x, z)$ into the wave equation, the bound-state eigenvalue equation is derived for spin-1 hadronic bound-state as

$$\left[-\frac{z}{e^{\varphi(z)}} \partial_z \left(\frac{e^{\varphi(z)}}{z} \partial_z \right) + \left(\frac{\mu R}{z} \right)^2 \right] \Phi(z) = M^2 \Phi(z). \quad (34)$$

Factoring out the scale \sqrt{z} and dilaton factors from the AdS field as $\Phi = \sqrt{\frac{z}{R}} e^{-\varphi(z)/2} \psi(z)$, and using the substitutes $z \rightarrow \zeta$, we find light-front Schroedinger equation (Eq. (29)) with effective potential $U(\zeta) = \frac{1}{2} \varphi''(\zeta) + \frac{1}{4} \varphi'(\zeta)^2 - \frac{1}{\zeta} \varphi'(\zeta)$, and the AdS mass $(\mu R)^2 = L^2 - 1$. In this correspondence, $\varphi(\zeta)$ and $(\mu R)^2$ are related to the effective potential and the internal orbital angular momentum L , respectively.

Choosing $\varphi(\zeta) = \kappa^2 \zeta^2$ in the soft-wall model [56] leads to $U(\zeta) = \kappa^4 \zeta^2$. Solving Eq. (29) with this potential and comparing the equation for the quantum mechanical oscillator in polar coordinates, we obtain the results in eigenfunctions and eigenvalues as $\psi(\zeta) = \kappa \sqrt{2\zeta} e^{-\frac{\kappa^2 \zeta^2}{2}}$ and $M^2 = 4\kappa^2 \left(n + \frac{1+L}{2} \right)$, respectively.

To determine the function $f(\alpha)$ in Eq. (28), we use the condition $\int_0^1 d\alpha \frac{f(\alpha)^2}{\alpha(1-\alpha)} = 1$ [28]. Therefore, $\phi_\lambda(r, \alpha)$ for K_{1A} state with massless quarks, and $n = 0$, $L = 0$ is obtained as

$$\phi_\lambda^{K_{1A}}(\alpha, \zeta) = \mathcal{N}_\lambda \frac{\kappa}{\sqrt{\pi}} \sqrt{\alpha(1-\alpha)} \exp \left(-\frac{\kappa^2 \zeta^2}{2} \right), \quad (35)$$

where $\kappa = M_{K_{1A}}/\sqrt{2}$. To include the light quark masses, we apply a Fourier transform to \mathbf{k} -space as $\tilde{\phi}(\alpha, \mathbf{k}_\perp) = \int d^2\mathbf{r} e^{-i\mathbf{k}_\perp \cdot \mathbf{r}} \phi(\alpha, \zeta)$, and obtain

$$\tilde{\phi}_\lambda^{K_{1A}}(\alpha, \mathbf{k}_\perp) = \mathcal{N}_\lambda \frac{2}{\sqrt{\alpha(1-\alpha)}} \frac{\sqrt{\pi}}{\kappa} \exp \left(-\frac{\mathbf{k}_\perp^2}{2\alpha(1-\alpha)\kappa^2} \right). \quad (36)$$

For massive quarks, we should replace [24]:

$$\frac{\mathbf{k}_\perp^2}{\alpha(1-\alpha)} \rightarrow \frac{\mathbf{k}_\perp^2}{\alpha(1-\alpha)} + \frac{m_u^2}{\alpha} + \frac{m_s^2}{(1-\alpha)}. \quad (37)$$

After substituting this into the wave function and Fourier transforming back to transverse position-space, one obtains the final form of the AdS/QCD wave function:

$$\phi_\lambda^{K_{1A}}(\zeta, \alpha) = \mathcal{N}_\lambda \frac{\kappa}{\sqrt{\pi}} \sqrt{\alpha(1-\alpha)} \exp\left(-\frac{\kappa^2 \zeta^2}{2}\right) \exp\left\{-\left[\frac{m_u^2 - \alpha(m_u^2 - m_s^2)}{2\alpha(1-\alpha)\kappa^2}\right]\right\}. \quad (38)$$

In position-space, \mathcal{N}_λ can be fixed by this normalization condition [50]:

$$\int d^2\mathbf{r} d\alpha \left[\sum_{h, \bar{h}} |\Psi_{h, \bar{h}}^{K_{1A}, \lambda}(r, \alpha)|^2 \right] = 1. \quad (39)$$

In the next section, we estimate the decay constants and DAs for $K_1(1270)$ and $K_1(1400)$ mesons. As an application of these DAs, we can use them to calculate the transition form factors of the semileptonic $B \rightarrow K_1(1270, 1400) \ell^+ \ell^-$ decays.

III. NUMERICAL ANALYSIS

In this section, we present our numerical analysis for the DAs of $K_1(1270, 1400)$ mesons in terms of the DAs of K_{1A} and K_{1B} states in the AdS/QCD correspondence. Then, the transition form factors of $B \rightarrow K_1 \ell^+ \ell^-$ decays are investigated. The other phenomenological quantities can be evaluated by using these form factors. In this paper, we take masses as: $m_b = (4.81 \pm 0.03)$ GeV, $m_B = (5.27 \pm 0.01)$ GeV [57], $m_{K_{1A}} = (1.31 \pm 0.06)$ GeV, and $m_{K_{1B}} = (1.34 \pm 0.08)$ GeV [3]. In addition, we choose light quark masses as $m_{u,d} = 350$ MeV and $m_s = 480$ MeV [39]. It should be noted that the values of the effective quark masses, used in the holographic LFWFs, are clearly different from the conventional constituent masses in the non-relativistic theories.

We obtain the decay constant values for K_{1A} and K_{1B} states from Eqs. (26) and (27) as presented in Table I. This table also contains the results obtained in the frame work of the LCSR [3]. As mentioned before, we take $f_{K_{1A}}^\perp = f_{K_{1A}}$, and $f_{K_{1B}} = f_{K_{1B}}^\perp$ in our analysis. Using Eq. (4) and values in Table I, we can evaluate the decay constant values for

TABLE I: Decay constant values of K_{1A} and K_{1B} states in MeV.

Approach	$f_{K_{1A}}$	$f_{K_{1B}}^\perp$
This work	236 ± 5	220 ± 5
LCSR [3]	250 ± 13	190 ± 10

mesons K_1 . In Table II, we compare our predictions for the decay constants of $K_1(1270)$ and $K_1(1400)$ mesons with those obtained using the LCSR approach at $\theta_K = -(34 \pm 13)^\circ$. The origin of a large error in calculation of the decay constants is due to the uncertainty in determination of the mixing angle.

TABLE II: Decay constant values of K_1 mesons (in MeV) compared to the LCSR at $\theta_K = -(34 \pm 13)^\circ$.

Approach	$f_{K_1(1270)}$	$f_{K_1(1270)}^\perp$	$f_{K_1(1400)}$	$f_{K_1(1400)}^\perp$
This work	-169 ± 39	144 ± 38	157 ± 35	172 ± 32
LCSR	-172 ± 43	117 ± 36	171 ± 35	159 ± 26

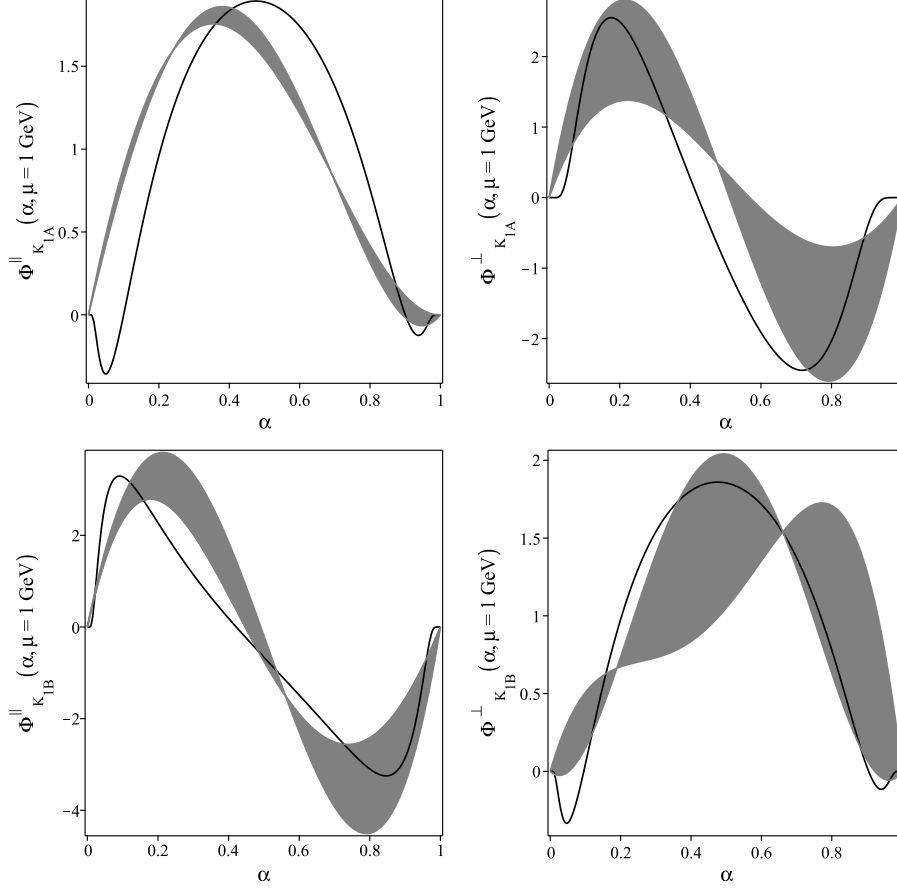
The approximate forms of the twist-2 DAs for K_{1A} and K_{1B} states in the frame work of the LCSR are as follows:

$$\Phi^{\parallel, \perp}(u) = 6u\bar{u} \left[a_0^{\parallel, \perp} + 3a_1^{\parallel, \perp} \xi + a_2^{\parallel, \perp} \frac{3}{2}(5\xi^2 - 1) \right], \quad (40)$$

where $\xi = 2u - 1$. The values of the Gegenbauer moments $a_i^{\parallel, \perp}$ $i = (0, 1, 2)$, for two states K_{1A} and K_{1B} have been estimated in Ref. [4] and given in Table III. Using Eqs. (19)-(22), and the decay constant values presented in Table II, we display our predictions for the twist-2 holographic LFDAs of K_{1A} and K_{1B} states at the scale $\mu = 1$ and $\mu = 2.2$ GeV in Figs. 1 and 2, respectively. In these figures, gray areas show the DAs predicted from the LCSR method for aforementioned states by considering their errors. In addition, we illustrate in Fig. 3 the two-parton

TABLE III: Gegenbauer moments of Φ_{\parallel} and Φ_{\perp} for K_{1A} and K_{1B} states.

μ	$a_0^{\parallel, K_{1A}}$	$a_1^{\parallel, K_{1A}}$	$a_2^{\parallel, K_{1A}}$	$a_0^{\perp, K_{1A}}$	$a_1^{\perp, K_{1A}}$	$a_2^{\perp, K_{1A}}$
1 GeV	1	$-0.30^{+0.00}_{-0.20}$	-0.05 ± 0.03	$0.27^{+0.03}_{-0.17}$	-1.08 ± 0.48	0.02 ± 0.20
2.2 GeV	1	$-0.25^{+0.00}_{-0.17}$	-0.04 ± 0.02	$0.25^{+0.03}_{-0.16}$	-0.88 ± 0.39	0.01 ± 0.15
	$a_0^{\parallel, K_{1B}}$	$a_1^{\parallel, K_{1B}}$	$a_2^{\parallel, K_{1B}}$	$a_0^{\perp, K_{1B}}$	$a_1^{\perp, K_{1B}}$	$a_2^{\perp, K_{1B}}$
1 GeV	-0.19 ± 0.07	-1.95 ± 0.45	$0.10^{+0.15}_{-0.19}$	1	$0.30^{+0.00}_{-0.33}$	-0.02 ± 0.22
2.2 GeV	-0.19 ± 0.07	-1.57 ± 0.37	$0.07^{+0.11}_{-0.14}$	1	$0.24^{0.00}_{-0.27}$	-0.02 ± 0.17

FIG. 1: The twist-2 DAs for K_{1A} and K_{1B} at $\mu = 1$ GeV in the AdS/QCD. Gray areas show the LCDAs by considering their errors.

DAs of twist-2 for $K_1(1270)$ and $K_1(1400)$ mesons at the scale $\mu = 1$ GeV in the frame work of the AdS/QCD and LCSR, where $\theta_K = -34^\circ$.

Now, the transition form factors of the semileptonic FCNC decays $B \rightarrow K_1(1270, 1400)$, which have been calculated in the LCSR approach [5], are evaluated using the holographic DAs. The explicit expressions of these transition form factors in terms of the DAs are given in Appendix. We find that, for $s_0 \simeq (33 \sim 36)$, all considered form factors in the AdS/QCD exhibit good stability within the Borel mass parameter $5 \text{ GeV}^2 \leq M^2 \leq 10 \text{ GeV}^2$. To evaluate the form factors in the physical region $4m_\ell^2 \leq q^2 \leq (m_B - m_{K_1})^2$, we fit the double-pole form

$$F_k(q^2) = \frac{F_k(0)}{1 - \alpha(q^2/m_B^2) + \beta(q^4/m_B^4)}, \quad (41)$$

for each form factor. In this fit function, we use the notation $F_k(q^2)$ to denote the form factors, $F_k(0)$, α and β are the corresponding coefficients and their values are presented in Table. IV at $\theta_K = -34^\circ$. We compare the AdS/QCD predictions for the transition form factors at $q^2 = 0$ with those of the LCSR in Table. V. As can be seen, there is a

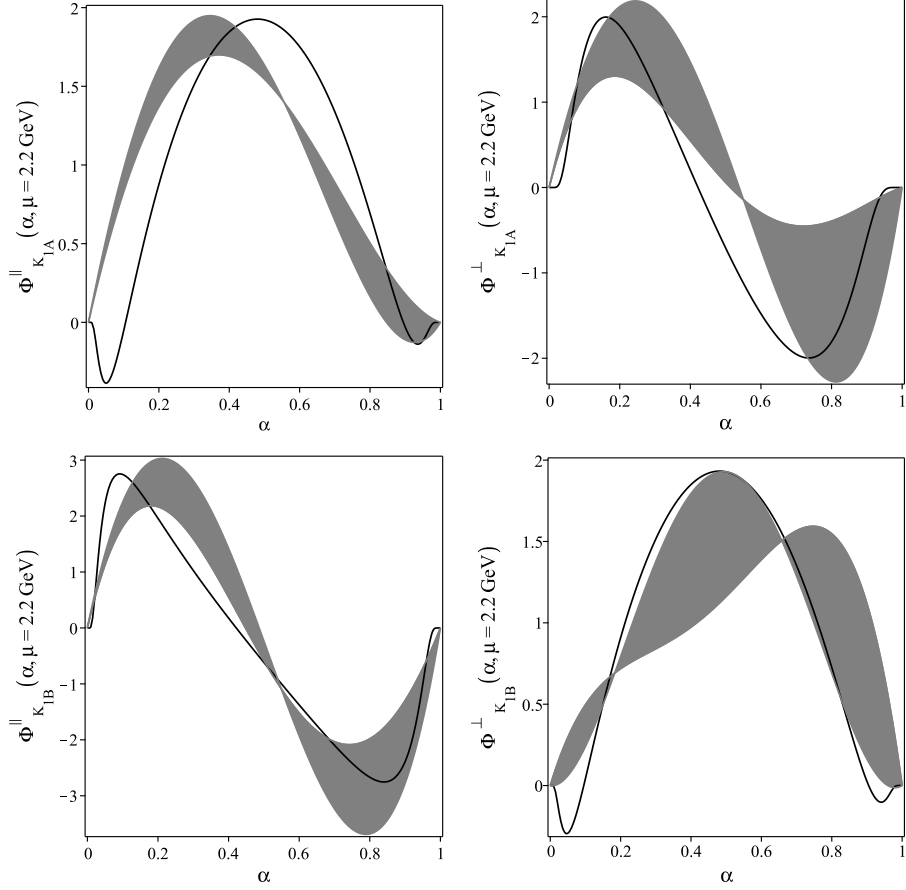


FIG. 2: The same as Fig. 1 but for $\mu = 2.2$ GeV.

TABLE IV: $F_k(0)$, α and β parameters for $B \rightarrow K_1(1270)[K_1(1400)]$ form factors using the holographic DAs in $\theta_K = -34^\circ$.

$F^{B \rightarrow K_1(1270)}$	$F(0)$	α	β	$F^{B \rightarrow K_1(1400)}$	$F(0)$	α	β
A	-0.60	1.49	0.59	A	0.12	2.01	1.41
V_0	0.29	2.14	1.20	V_0	-0.29	2.40	1.58
V_1	-0.45	0.84	0.10	V_1	0.13	0.77	1.76
V_2	-0.39	0.90	0.55	V_2	0.20	1.93	1.72
T_1	-0.37	2.64	1.92	T_1	0.11	1.12	1.01
T_2	-0.36	0.94	-0.18	T_2	0.10	2.43	1.89
T_3	-0.22	-0.15	-0.99	T_3	0.14	2.17	1.93

logical agreement between the AdS/QCD and LCSR predictions.

For a better analysis, we can illustrate the form factors of $B \rightarrow K_1(1270)$ and $B \rightarrow K_1(1400)$ transitions on q^2 in the AdS/QCD and LCSR methods. For instance, Fig. 4 shows the form factors A and T_1 in $\theta_K = -34^\circ$ via the AdS/QCD and LCSR approaches.

We would like to plot the differential branching ratios for $B \rightarrow K_1 \ell^+ \ell^-$ decays with respect to q^2 . The expression of double differential decay rate $d^2\Gamma/dq^2 d\cos\theta_\ell$ for $B \rightarrow K_1$ transitions can be found in Refs. [58, 59]. This expression contains the Wilson coefficients, the CKM matrix elements, the form factors related to the fit functions, series of functions and constants. The numerical values of the Wilson coefficients are taken from Ref. [60]. The other parameters can be found in Ref. [59]. After numerical analysis, the dependency of the differential branching ratios on q^2 , by considering the long distance (LD) effects, is shown in Fig. 5 in the $\theta_K = -34^\circ$. The LD is associated with real $c\bar{c}$ resonances in the intermediate states, i.e., the cascade process $B \rightarrow K_1 J/\psi(\psi') \rightarrow K_1 \ell^+ \ell^-$. Fig. 5 also contains the LCSR and Z' model predictions [16]. It is noted that the results for the non-universal Z' model are depicted in

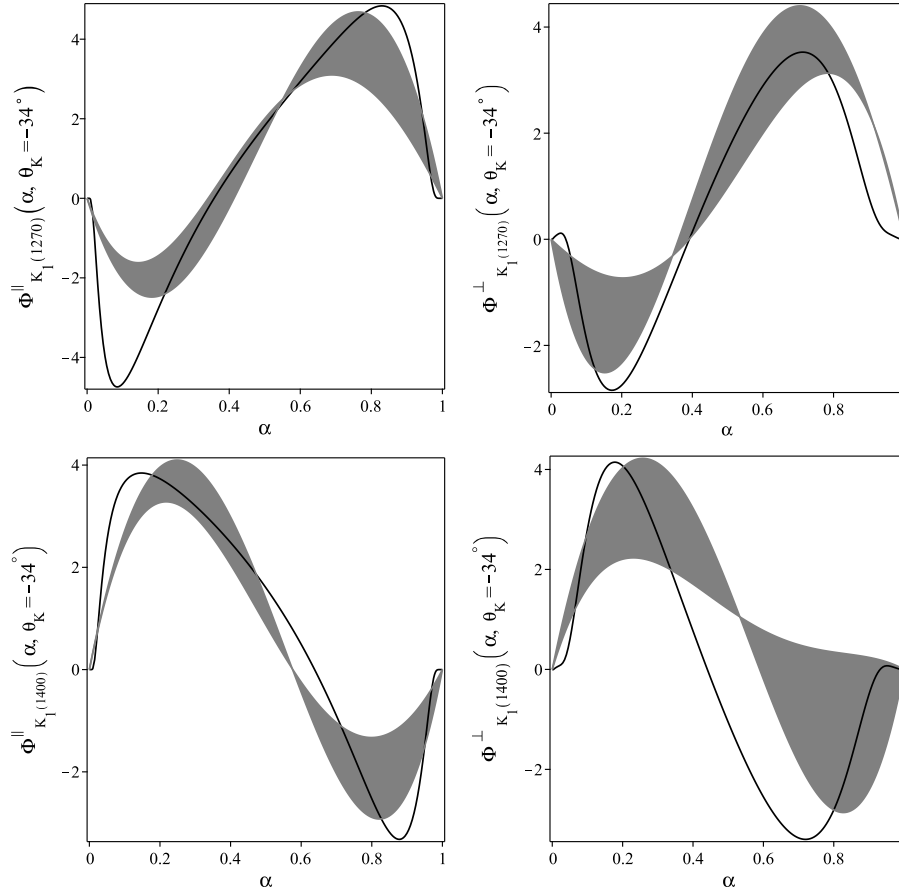


FIG. 3: The twist-2 DAs for $K_1(1270)$ and $K_1(1400)$ mesons at $\mu = 1$ GeV and $\theta_K = -34^\circ$ in the AdS/QCD. Gray areas show the LCDAs by considering their errors.

TABLE V: Our predictions for the form factors in $q^2 = 0$ compared to the LCSR predictions in $\theta_K = -34^\circ$.

$B \rightarrow K_1(1270)$	AdS/QCD	LCSR	$B \rightarrow K_1(1400)$	AdS/QCD	LCSR
A	-0.60 ± 0.08	-0.66 ± 0.13	A	0.11 ± 0.02	0.14 ± 0.03
V_0	0.29 ± 0.03	0.24 ± 0.04	V_0	-0.29 ± 0.02	-0.22 ± 0.04
V_1	-0.45 ± 0.06	-0.47 ± 0.08	V_1	0.13 ± 0.02	0.18 ± 0.03
V_2	-0.39 ± 0.04	-0.39 ± 0.06	V_2	0.20 ± 0.02	0.30 ± 0.05
T_1	-0.37 ± 0.03	-0.41 ± 0.05	T_1	0.11 ± 0.02	0.10 ± 0.02
T_2	-0.36 ± 0.03	-0.40 ± 0.05	T_2	0.10 ± 0.02	0.11 ± 0.02
T_3	-0.22 ± 0.02	-0.26 ± 0.04	T_3	0.14 ± 0.03	0.16 ± 0.04

three sets, considering only the short distance (SD) effect without the LD effects (for more details, see Ref. [16]). As can be seen, there is some difference between the predictions of the AdS/QCD and LCSR on one side and the Z' model, as a method beyond the standard model, on the other.

Our predictions for the branching ratio values of $B \rightarrow K_1 \ell^+ \ell^-$ decays at $\theta_K = -34^\circ$ are presented in Table VI.

To evaluate the branching ratio of the non-leptonic $B \rightarrow K_1(1270, 1400) \gamma$ decays, we use the exclusive decay width as [61]:

$$\Gamma(B \rightarrow K_1 \gamma) = \frac{\alpha_{em} G_F^2}{32\pi^4} m_b^5 |V_{tb} V_{ts}^*|^2 |C_7(m_b)|^2 (T_1(0)^{B \rightarrow K_1})^2 \left(1 - \frac{m_{K_1}^2}{m_B^2}\right)^3 \left(1 + \frac{m_{K_1}^2}{m_B^2}\right).$$

Table VII shows our predictions for the branching ratios of these exclusive non-leptonic decays at $\theta_K = -34^\circ$. The AdS/QCD prediction for the branching ratio of the $B \rightarrow K_1(1270) \gamma$ decay is larger than the experimental value that

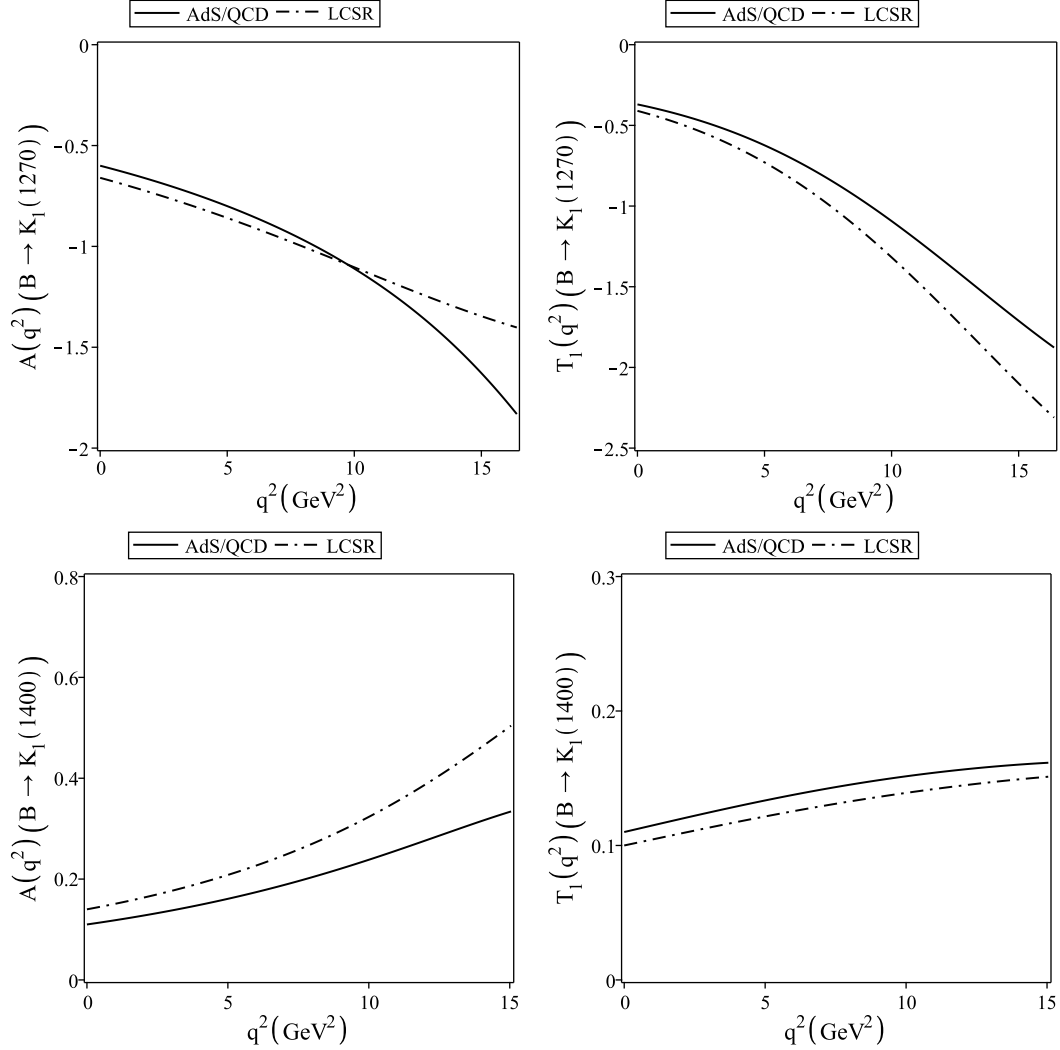


FIG. 4: The semileptonic form factors $A(q^2)$ and $T_1(q^2)$ for $B \rightarrow K_1(1270)$ and $B \rightarrow K_1(1400)$ transitions on q^2 in the AdS/QCD and LCSR methods.

TABLE VI: Branching ratio values of $B \rightarrow K_1(1270)\ell^+\ell^-$ decays at $\theta_K = -34^\circ$ in the AdS/QCD correspondence and LCSR model.

Mode	AdS/QCD	LCSR
$\text{Br}(B \rightarrow K_1(1270)\mu^+\mu^-) \times 10^6$	3.12 ± 1.14	2.91 ± 1.32
$\text{Br}(B \rightarrow K_1(1270)\tau^+\tau^-) \times 10^7$	1.25 ± 0.53	1.07 ± 0.45
$\text{Br}(B \rightarrow K_1(1400)\mu^+\mu^-) \times 10^7$	1.13 ± 0.41	0.90 ± 0.33
$\text{Br}(B \rightarrow K_1(1400)\tau^+\tau^-) \times 10^9$	1.15 ± 0.92	1.11 ± 0.90

is $(0.43 \pm 0.18) \times 10^{-4}$ [62]. However, our estimation has many errors due to the uncertainties in the mixing angle θ_K .

Finally, we plot dependence of the forward-backward asymmetries, A_{FB} , on q^2 for $B \rightarrow K_1(1270, 1400)\ell^+\ell^-$ decays, by considering the LD effects, at $\theta_K = -34^\circ$ in Fig. 6. Gray regions show the errors of the AdS/QCD correspondences due to the uncertainties of the input parameters. In this figure, we also present the behavior of the forward-backward asymmetries with respect to q^2 in the frame work of the 2HDM as a NP model. To draw the 2HDM diagrams, we insert the AdS/QCD form factors in the 2HDM formalism for three cases A, B and C related to λ_{tt} and λ_{bb} (for more details, see Ref. [15]) in order to compare the AdS/QCD and 2HDM results.

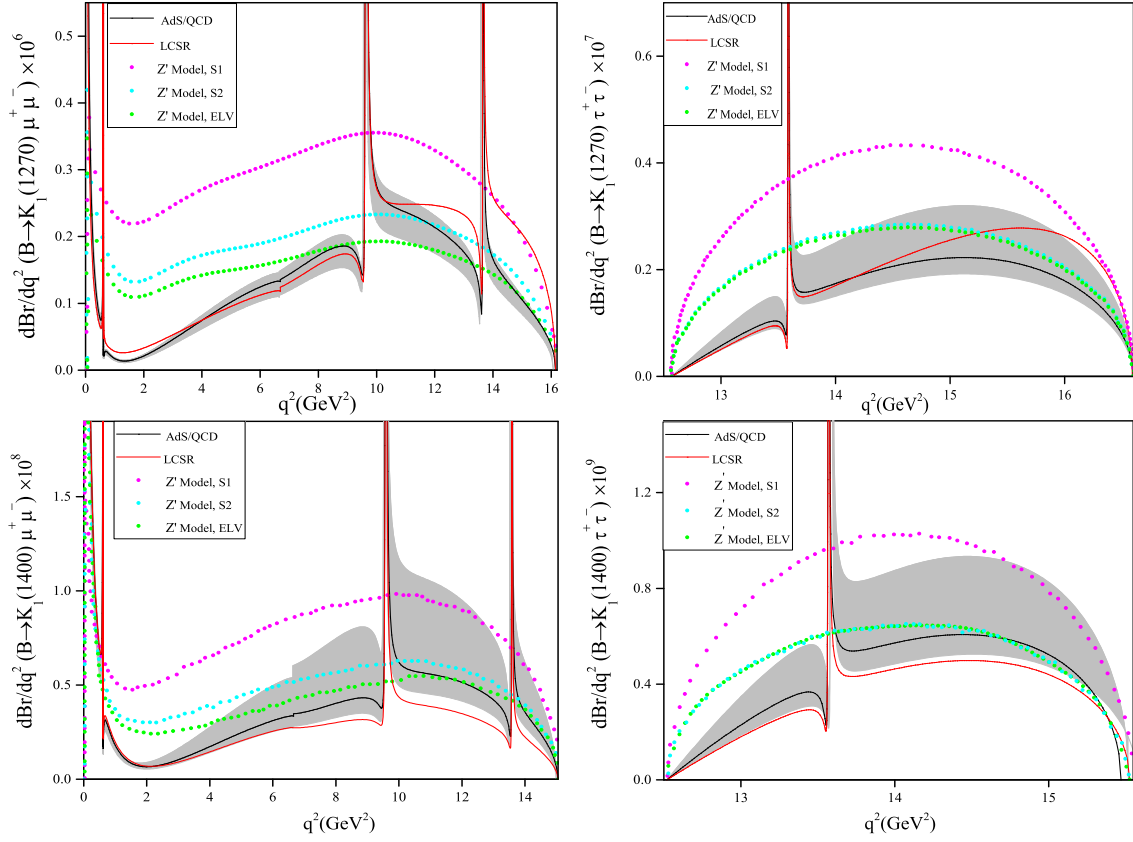


FIG. 5: The differential branching ratios of the semileptonic $B \rightarrow K_1 \ell^+ \ell^-$ decays for $\ell = \mu, \tau$ on q^2 via the AdS/QCD in comparison with the LCSR and Z' model.

TABLE VII: AdS/QCD predictions for the branching ratios of $B \rightarrow K_1(1270, 1400)\gamma$ decays in $\theta_K = -34^\circ$.

Mode	AdS/QCD	EXP [62]
$\text{Br}(B \rightarrow K_1(1270)\gamma) \times 10^4$	0.71 ± 0.23	0.43 ± 0.18
$\text{Br}(B \rightarrow K_1(1400)\gamma) \times 10^5$	1.56 ± 1.04	< 1.44

As can be seen in Fig. 6, the forward-backward asymmetries for $B \rightarrow K_1(1270, 1400)\tau^+\tau^-$ transitions are positive for all values of q^2 except in the resonance region. On the other hand, the 2HDM plots are out of the AdS/QCD predictions and its errors. Therefor, their investigation in experiments will be a very efficient tool in establishing a new physics.

In summary, we used the AdS/QCD correspondence as a new remarkable feature of the light-front holography, to derive the non-perturbative twist-2 DAs and decay constants for the pure axial-vector states, K_{1A} and K_{1B} . The holographic DAs for $K_1(1270)$ and $K_1(1400)$ mesons were calculated in terms of the DAs for the aforementioned states. Using the holographic DAs for $K_1(1270, 1400)$ mesons, we evaluated transition form factors of the FCNC $B \rightarrow K_1(1270, 1400)\ell^+\ell^-$ decays. A comparison was made between our results and the LCSR predictions for the twist-2 DAs, decay constants and form factors. We presented our results for the branching ratio values of the leptonic $B \rightarrow K_1(1270, 1400)\ell^+\ell^-$, ($\ell = \mu, \tau$), and non-leptonic $B \rightarrow K_1(1270, 1400)\gamma$ decays at the mixing angle $\theta_K = -34^\circ$. The AdS/QCD prediction for the branching ratio of the $B \rightarrow K_1(1270)\gamma$ decay is larger than the experimental value. Finally, considering the LD effects, we showed the dependence of the forward-backward asymmetries A_{FB} on q^2 for $B \rightarrow K_1(1270, 1400)\ell^+\ell^-$ decays at $\theta_K = -34^\circ$ in the framework of the AdS/QCD and 2HDM. Since there was not an overlap between the results of $A_{FB}(B \rightarrow K_1(1270, 1400)\tau^+\tau^-)$ from two theories, their experimental investigation can serve as a crucial test in search of new physics.

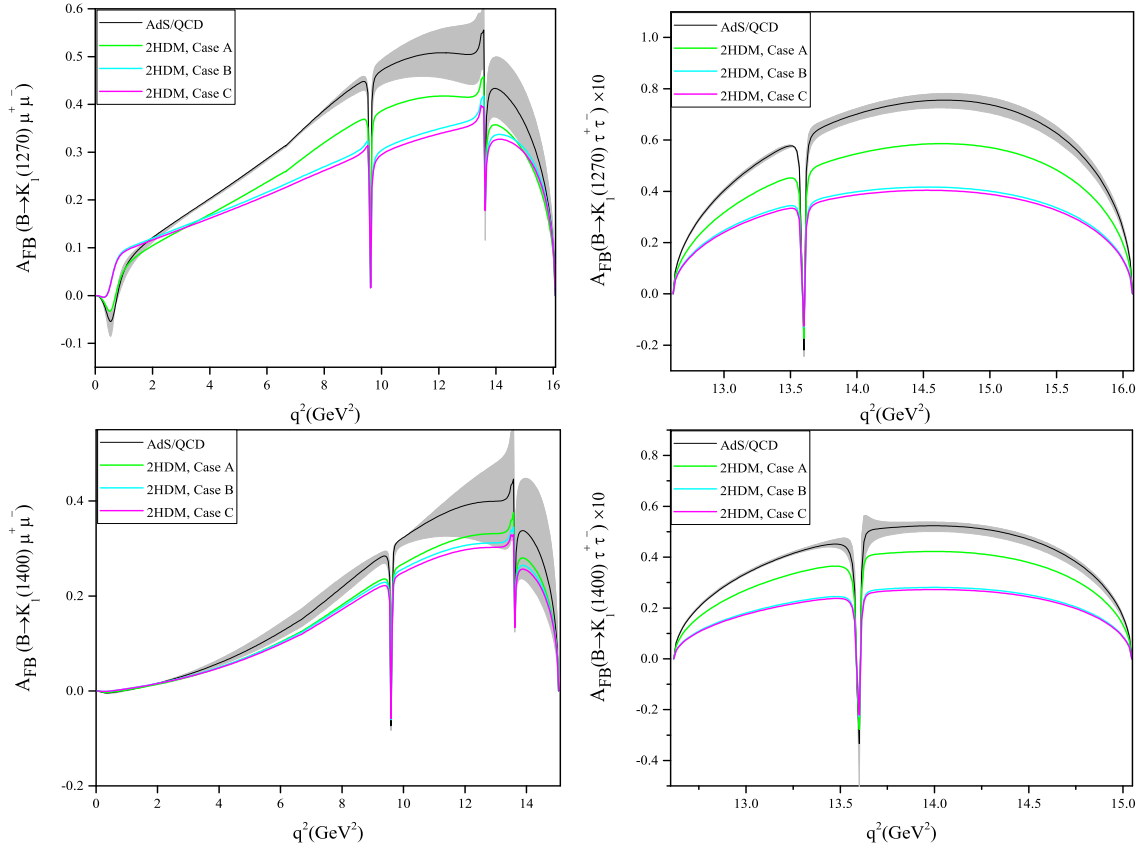


FIG. 6: Dependence of the forward-backward asymmetries for $B \rightarrow K_1 \ell^+ \ell^-$ ($\ell = \mu, \tau$) decays on q^2 with the AdS/QCD, LCSR and 2HDM approaches. Gray areas show the errors of the AdS/QCD correspondence.

Acknowledgments

Partial support from the Isfahan university of technology research council is appreciated.

Appendix: Expressions for the form factors

In this appendix, the explicit expressions for the form factors of the FCNC $B \rightarrow K_1(1270, 1400) \ell^+ \ell^-$ decays are presented.

$$\begin{aligned}
A(q^2) &= \frac{f_A m_b}{4 m_B^2 f_B} (m_A - m_B) \left\{ \frac{f_A^\perp}{f_A} \int_{u_0}^1 du \frac{9 \Phi^\perp(u)}{u} e^{s(u)} + \frac{m_b}{4 m_A} \int_{u_0}^1 du \frac{g_\perp^{(v)'}(u)}{u} e^{s(u)} \right. \\
&\quad \left. - \frac{m_b}{4 m_A} \int_{u_0}^1 du \frac{g_\perp^{(v)}(u)}{u^2} \left[1 + \frac{\delta_1(u) - 8 m_A^2}{M^2} \right] e^{s(u)} + \frac{f_A^\perp m_A^2}{f_A} \int_{u_0}^1 du \frac{32 \bar{h}_\parallel^{(t)(ii)}(u)}{M^2} e^{s(u)} \right\}, \\
V_1(q^2) &= -\frac{m_b}{8 m_B^2 f_B} \frac{f_A^\perp}{(m_B - m_A)} \left\{ \frac{1}{2} \int_{u_0}^1 du \frac{7 \Phi^\perp(u) \delta_1(u)}{u} e^{s(u)} + 2 m_A^2 \int_{u_0}^1 du \frac{h_\parallel^{(p)}(u)}{u} e^{s(u)} \right. \\
&\quad \left. - 3 \frac{f_A}{f_A^\perp} m_A m_b \int_{u_0}^1 du \frac{g_\perp^{(a)}(u)}{u} e^{s(u)} - 8 m_A^2 \int_{u_0}^1 du \frac{\bar{h}_\parallel^{(t)(ii)}(u)}{u^2} e^{s(u)} \right\}, \\
V_2(q^2) &= -\frac{f_A^\perp m_b}{4 m_B^2 f_B} (m_B - m_A) \left\{ 18 \int_{u_0}^1 du \frac{\Phi^\perp(u)}{u} e^{s(u)} + \frac{4 f_A m_A m_B}{f_A^\perp} \int_{u_0}^1 du \frac{\phi_a(u)}{u^2 M^2} e^{s(u)} \right. \\
&\quad + 4 m_A^2 \int_{u_0}^1 du \frac{h_\parallel^{(p)}(u)}{u} (1 + 2u) e^{s(u)} + \frac{16 f_A}{f_A^\perp} m_A m_b \int_{u_0}^1 du \frac{\Phi^\parallel(i)(u)}{u^2 M^2} e^{s(u)} \\
&\quad \left. - 16 m_A^2 \int_{u_0}^1 du \frac{\bar{h}_\parallel^{(t)(ii)}(u)}{u^2} \left[\frac{2 \delta_3(u)}{u M^4} - \frac{3}{2 M^2} \frac{\delta_1(u)}{4 u M^4} \right] e^{s(u)} \right\}, \\
V_0(q^2) &= V_3(q^2) + \frac{m_b}{8 m_B^2 f_B} \frac{f_A^\perp q^2}{m_A} \left\{ 9 \int_{u_0}^1 du \frac{\Phi^\perp(u)}{u} e^{s(u)} + 2 f_A m_A m_B \int_{u_0}^1 du \frac{\phi_a(u)}{u^2 M^2} e^{s(u)} \right. \\
&\quad - 4 m_A^2 \int_{u_0}^1 du \frac{h_\parallel^{(p)}(u)}{u} (1 - u) e^{s(u)} + \frac{16 f_A}{f_A^\perp} m_A m_b \int_{u_0}^1 du \frac{\Phi^\parallel(i)(u)}{u^2 M^2} e^{s(u)} \\
&\quad \left. + 8 m_A^2 \int_{u_0}^1 du \frac{\bar{h}_\parallel^{(t)(ii)}(u)}{u^2} \left[\frac{2 \delta_3(u)}{u M^4} - \frac{1}{M^2} + (1 - u) \left(-\frac{1}{M^2} + \frac{\delta_1(u)}{2 u M^4} \right) \right] e^{s(u)} \right\}, \\
T_1(q^2) &= -\frac{f_A m_b}{8 m_B^2 f_B} \left\{ m_b \left(\frac{f_A^\perp}{f_A} + 8 \right) \int_{u_0}^1 du \frac{\Phi^\perp(u)}{u} e^{s(u)} - 3 m_A \int_{u_0}^1 du g_\perp^{(a)}(u) e^{s(u)} \right. \\
&\quad + 4 m_A \int_{u_0}^1 du \frac{\phi_a(u)}{u} e^{s(u)} - \frac{f_A}{m_A} \int_{u_0}^1 du \frac{g_\perp^{(v)'}(u) \delta_5(u)}{u} e^{s(u)} - \frac{m_A}{8} \int_{u_0}^1 du \frac{g_\perp^{(v)'}(u)}{u} \\
&\quad \times \left[7 - \frac{\delta_5(u)(8u - 1)}{M^2} + \frac{u \delta_2(u) - \delta_4(u)}{2 m_A^2} \right] e^{s(u)} + 4 m_A \int_{u_0}^1 du \frac{\Phi^\parallel(i)(u)}{u} e^{s(u)} - \frac{16 f_A^\perp}{f_A} \\
&\quad \times m_A^2 m_b \int_{u_0}^1 du \frac{\bar{h}_\parallel^{(t)(ii)}(u)}{u M^2} e^{s(u)} \left. \right\}, \\
T_2(q^2) &= \frac{m_b}{m_B^2 f_B} \frac{f_A}{m_A^2 - m_B^2} \left\{ \frac{m_b f_A^\perp}{f_A} \int_{u_0}^1 du \frac{\Phi^\perp(u) \delta_1(u)}{u} e^{s(u)} + \frac{1}{2} m_A \int_{u_0}^1 du \frac{g_\perp^{(a)}(u)}{u} \right. \\
&\quad \times [\delta_1(u) + 4 \delta_5(u)] e^{s(u)} - \frac{1}{16} m_A \int_{u_0}^1 du \frac{g_\perp^{(v)'}(u) \delta_2(u)}{u} e^{s(u)} + \frac{1}{2} m_A \int_{u_0}^1 du \frac{\phi_a(u)}{u} \\
&\quad \times \delta_1(u) e^{s(u)} + m_A \int_{u_0}^1 du \frac{g_\perp^{(v)}(u)}{u^2} \left[\delta_6(u) + \frac{\delta_1(u) \delta_5(u)}{M^2} + \frac{u \delta_2(u)}{2} \left(1 + \frac{\delta_3(u)}{u M^2} + \frac{\delta_7(u)}{u} \right) \right. \\
&\quad \left. + u \left(m_A^2 - 2 \delta_1(u) + \frac{\delta_4(u)}{2} + \frac{\delta_5(u) \delta_1(u)}{u M^2} \right) \right] e^{s(u)} - 2 m_A \int_{u_0}^1 du \frac{\Phi^\parallel(i)(u) \delta_2(u)}{u} e^{s(u)} \\
&\quad \left. - 8 \frac{f_A^\perp}{f_A} m_A^2 m_b \int_{u_0}^1 du \frac{\bar{h}_\parallel^{(t)(ii)}(u)}{u^2} \left[1 + \frac{\delta_2(u)}{M^2} \right] e^{s(u)} \right\},
\end{aligned}$$

$$\begin{aligned}
T_3(q^2) = & -\frac{f_A m_b}{4 m_B^2 f_B} \left\{ \frac{8 f_A^\perp}{f_A} m_b \int_{u_0}^1 du \frac{\Phi^\perp(u)}{u} e^{s(u)} - 4 m_A \int_{u_0}^1 du \frac{g_\perp^{(a)}(u)}{u} e^{s(u)} - \frac{1}{4 m_A} \right. \\
& \times \int_{u_0}^1 du \frac{g_\perp^{(v)'}(u)}{u} \left[\frac{7}{2} \delta_2(u) + m_A^2 - \frac{\delta_1(u)}{4 u} \right] e^{s(u)} - m_A \int_{u_0}^1 du \frac{\phi_a(u)}{u^2} \left[\frac{u \delta_1(u) + 2 \delta_2(u)}{M^2} \right. \\
& + \left. \frac{1}{u} \right] e^{s(u)} - 4 m_A \int_{u_0}^1 du \frac{\Phi^{\parallel(i)}(u)}{u^2} \left[\frac{u \delta_5(u) - \delta_2(u)}{M^2} - 1 \right] e^{s(u)} - \frac{1}{4 m_A} \int_{u_0}^1 du \frac{g_\perp^{(v)}(u)}{u} \\
& \times \left[\frac{3 \delta_1(u)}{u M^2} - \frac{\delta_1(u)}{m_{a_1}^2} + \frac{5 \delta_5(u) - 7 \delta_3(u)}{M^2} + \frac{\delta_2(u)}{M^2} - \frac{\delta_1(u)^2}{m_{a_1}^2 M^2} \right] e^{s(u)} + \frac{16 f_A^\perp}{f_A} m_A^2 m_b \\
& \times \left. \int_{u_0}^1 du \frac{\bar{h}_\parallel^{(t)(ii)}(u)}{u^2 M^2} \left[8 + \frac{2}{u} + \frac{\delta_2(u)}{u M^2} \right] e^{s(u)} \right\},
\end{aligned}$$

where

$$\begin{aligned}
u_0 &= \frac{1}{2 m_A^2} \left[\sqrt{(s_0 - m_A^2 - q^2)^2 + 4 m_A^2 (m_b^2 - q^2)} - (s_0 - m_A^2 - q^2) \right], \\
s(u) &= -\frac{1}{u M^2} [m_b^2 + u \bar{u} m_A^2 - \bar{u} q^2] + \frac{m_B^2}{M^2}, \\
\delta_1(u) &= m_A^2 (u + 2) + \frac{m_b^2}{u} + \frac{q^2}{u}, \quad \delta_2(u) = u m_A^2 - \frac{m_b^2}{u} + q^2 \frac{u - \bar{u}}{u}, \\
\delta_3(u) &= \frac{m_b^2}{u} - 2 q^2 \frac{\bar{u}}{u}, \quad \delta_4(u) = 2 m_A^2 (u + 1) + 2 q^2, \\
\delta_5(u) &= u m_A^2 - \frac{m_b^2}{u} + \frac{q^2 (u - 2)}{u}, \quad \delta_6(u) = 2 m_A^2 (u + 1) + q^2 \frac{\bar{u}}{u}, \\
\delta_7(u) &= -2 \frac{m_b^2}{u} + \frac{q^2}{u}, \quad f^{(i)}(u) \equiv \int_0^u f(v) dv, \\
f^{(ii)}(u) &\equiv \int_0^u dv \int_0^v d\omega f(\omega), \quad \bar{h}_\parallel^{(t)} = h_\parallel^{(t)} - \frac{1}{2} \Phi^\perp(u), \\
\phi_a(u) &= \int_0^u [\Phi^\parallel - g_\perp^{(a)}(v)] dv.
\end{aligned}$$

-
- [1] H. Dag, A. Ozpineci and M. T. Zeyrek, J. Phys. G **38**, 015002 (2011).
 - [2] M. Bayar and K. Azizi, Eur. Phys. J. C **61**, 401 (2009).
 - [3] K. C. Yang, Nucl. Phys. B **776**, 187 (2007).
 - [4] K. C. Yang, Phys. Rev. D **78**, 034018 (2008).
 - [5] S. Momeni and R. Khosravi, Phys. Rev. D **95**, 016009 (2017).
 - [6] R. H. Li, C. D. Lu and W. Wang, Phys. Rev. D **79**, 034014 (2009).
 - [7] R. H. Li, C. D. Lu and W. Wang, Phys. Rev. D **79**, 094024 (2009).
 - [8] H. Y. Cheng and C. K. Chua, Phys. Rev. D **81**, 114006 (2010).
 - [9] R. C. Verma, arXiv:1103.2973 [hep-ph].
 - [10] I. Ahmed, M. A. Paracha and M. J. Aslam, Eur. Phys. J. C **54**, 591 (2008).
 - [11] A. Saddique, M. J. Aslam and C. D. Lu, Eur. Phys. J. C **56**, 267 (2008).
 - [12] I. Ahmed, M. A. Paracha and M. J. Aslam, Eur. Phys. J. C **71**, 1521 (2011).
 - [13] V. Bashiry and K. Azizi, JHEP **1001**, 033 (2010).
 - [14] A. Ahmed, I. Ahmed, M. A. Paracha and A. Rehman, Phys. Rev. D **84** 033010 (2011).
 - [15] F. Falahati and A. Zahedidareshouri, Phys. Rev. D **90**, 075002 (2014).
 - [16] Y. Li, J. Hua and K. C. Yang, Eur. Phys. J. C **71**, 1775 (2011).
 - [17] H. Hatanaka and K. C. Yang, Phys. Rev. D **78**, 074007 (2008).
 - [18] J. M. Maldacena, Adv. Theor. Math. Phys. **2**, 231 (1998).
 - [19] J. M. Maldacena, Int. J. Theor. Phys. **38**, 1113 (1999).
 - [20] S. J. Brodsky and G. F. de Teramond, Phys. Lett. B **582**, 211 (2004).
 - [21] G. F. de Teramond and S. J. Brodsky, Phys. Rev. Lett. **94**, 201601 (2005).

- [22] S. J. Brodsky and G. F. de Teramond, Phys. Rev. Lett. **96**, 201601 (2006).
- [23] S. J. Brodsky and G. F. de Teramond, Phys. Rev. D **77**, 056007 (2008).
- [24] S. J. Brodsky and G. F. de Teramond, arXiv: 0802.0514 [hep-ph].
- [25] S. J. Brodsky and G. F. de Teramond, Phys. Rev. D **78**, 025032 (2008).
- [26] A. Deur, V. Burkert, J. P. Chen and W. Korsch, Phys. Lett. B **665**, 349 (2008).
- [27] S. J. Brodsky and R. Shrock, Phys. Lett. B **666**, 95 (2008).
- [28] G. F. de Teramond and S. J. Brodsky, Phys. Rev. Lett. **102**, 081601 (2009).
- [29] S. Hong, S. Yoon and M. J. Strassler, JHEP **0604**, 003 (2006).
- [30] A. V. Radyushkin, Phys. Lett. B **642**, 459 (2006).
- [31] H. R. Grigoryan and A.V. Radyushkin, Phys. Lett. B **650**, 421 (2007).
- [32] H. R. Grigoryan and A.V. Radyushkin, Phys. Rev. D **76**, 095007 (2007).
- [33] J. R. Forshaw and R. Sandapen, Phys. Rev. Lett. **109**, 081601 (2012).
- [34] T. Branz, T. Gutsche, V. E. Lyubovitskij, I. Schmidt and A. Vega, Phys. Rev. D **82**, 074022 (2010).
- [35] C. W. Hwang, Phys. Rev. D **86**, 014005 (2012).
- [36] M. Ahmady and R. Sandapen, Phys. Rev. D **87**, 054013 (2013).
- [37] M. Ahmady and R. Sandapen, Phys. Rev. D **88**, 014042 (2013).
- [38] M. Ahmady, R. Campbell, S. Lord and R. Sandapen, Phys. Rev. D **88**, 074031 (2013).
- [39] M. Ahmady, R. Campbell, S. Lord and R. Sandapen, Phys. Rev. D **88**, 014042 (2014).
- [40] M. R. Ahmady, S. Lord and R. Sandapen, Phys. Rev. D **90**, 074010 (2014).
- [41] M. Ahmady, S. Lord and R. Sandapen, Nucl. Part. Phys. Proc. **273** (2016).
- [42] M. Ahmady, F. Chishtie and R. Sandapen, Phys. Rev. D **95**, 074008 (2017).
- [43] Q. Chang, S. J. Brodsky and X.Q. Li, Phys. Rev. D **95**, 094025 (2017).
- [44] S. Momeni and R. Khosravi, Phys. Rev. D **97**, 056005 (2018).
- [45] H. Yang et al., Phys. Rev. Lett. **94**, 111802 (2005).
- [46] L. Burakovsky and T. Goldman, Phys. Rev. D **57**, 2879 (1998).
- [47] M. Suzuki, Phys. Rev. D **47**, 1252 (1993).
- [48] H. Y. Cheng, Phys. Rev. D **67**, 094007 (2003).
- [49] H. Hatanaka, K. C. Yang, Phys. Rev. D **77**, 094023 (2008).
- [50] J. R. Forshaw and R. Sandapen, JHEP **1110**, 093 (2011).
- [51] J. B. Kogut and L. Susskind, Phys. Rev. D **9**, 3391 (1974).
- [52] M. Diehl, Eur. Phys. J. C **25**, 223 (2002).
- [53] G. P. Lepage and S. J. Brodsky, Phys. Rev. D **22**, 2157 (1980).
- [54] S. Wandzura and F. Wilczek, Phys. Lett. B **82**, 195 (1977).
- [55] S. J. Brodsky, G. F. de Teramond, H. G. Dosch and J. Erlich, arXiv: 1407.8131 [hep-ph].
- [56] A. Karch, E. Katz, D. T. Son, and M. A. Stephanov, Phys. Rev. D **74**, 015005 (2006).
- [57] C. Patrignani et al. (Particle Data Group), Chin. Phys. C **40**, 100001 (2016).
- [58] C. Q. Geng and C. C. Liu, J. Phys. G **29**, 1103 (2003).
- [59] P. Colangelo, F. De Fazio, P. Santorelli and E. Scrimieri, Phys. Rev. D **53**, 3672 (1996).
- [60] A. Ali, P. Ball, L.T. Handoko and G. Hiller, Phys. Rev. D **61** 074024 (2000).
- [61] A. S. Safir, Eur. Phys. J. C **3**, 15 (2001).
- [62] H. Yang et al., Phys. Rev. Lett. **94**, 111802 (2005).